

P–H activation of secondary phosphanes on a
parent amido diiridium complex†‡Cite this: *Dalton Trans.*, 2014, **43**,
1609Inmaculada Mena,^a Miguel A. Casado,^{*a} Víctor Polo,^b Pilar García-Orduña,^a
Fernando J. Lahoz^a and Luis A. Oro^{*a,c}

Selected secondary phosphanes (H–PR₂; R = Ph, Cy, ⁱPr) smoothly react with a parent amido-bridged diiridium cyclooctadiene complex affording mixed amido/(bis)phosphido dinuclear species. A careful investigation of the reaction profile, carried out by experimental and theoretical tools, revealed that, after an initial amido/phosphido exchange, at low temperatures a second molecule of secondary phosphane adds to the dinuclear system through an oxidative addition process leading to a hydrido amido/bis(phosphido) mixed-valence complex [Ir^{III}/Ir^I]. These species rearrange above –10 °C into the most stable isomer that arises from a migration of the hydrido moiety to one of the =CH fragments of a coordinated cod molecule, a transformation facilitated by the formation of an intermetallic bond. Further heating of these species reductively eliminates ammonia affording bis(phosphido)-metal–metal bonded complexes.

Received 15th October 2013,
Accepted 18th October 2013

DOI: 10.1039/c3dt52911h

www.rsc.org/dalton

Introduction

Metal–metal interactions on dinuclear complexes often rely on the architecture of the bridging ligands that support the metallic assemblies, that is, their size and flexibility.¹ While the size of a given bridging ligand establishes the proximity of the metal centres, its flexibility is a key factor determining the possibility of approach between the metals and the establishment of intermetallic interactions, so that cooperative reactivity may in principle be an issue to consider.² In this context, the ability of –SR,³ –OR⁴ and –NHR⁵ moieties to efficiently behave as bridging ligands towards late metals is known, as they are highly flexible to allow a wide range of intermetallic separations, a situation that opens the possibility of metal–metal bonding.

Among the series of these heteroatom-based anions, the simplest nitrogen-based one is the parent-amido (–NH₂) ligand, which has drawn a great deal of attention in the last few years and is able to stabilize a number of different

dinuclear assemblies by bridging both metals quite tightly.⁶ Late transition metal parent–amido complexes are extremely rare; however, they are emerging as quite relevant species in the most recent organometallic chemistry. Their interest emerges from two distinct perspectives: (i) the activation of ammonia as a source of amido ligands;^{7,8} under this idea, new imaginative methodologies that utilize raw ammonia directly to prepare amido complexes have been reported, an approach that may eventually drive metal-mediated functionalization of ammonia;⁹ and (ii) the non-innocent behaviour of the amido ligands, a phenomenon that is beginning to be disclosed and influences the reactivity and catalytic properties of amido complexes.¹⁰ In this line, a significant contribution has been recently reported dealing with the role of [Ir–NH₂–Ir] linkages in catalytic transfer hydrogenation, indicating a novel binuclear, outer-sphere Noyori-like mechanism, which illustrates the key role of NH₂ groups in alcohol dehydrogenation and imido formation.¹¹

Herein we report on the activation of P–H bonds of selected secondary phosphanes by a parent-amido bridged diiridium cyclooctadiene complex, which leads to rare parent amido/phosphido-bridged complexes and ultimately to bis(phosphido) bridged metal–metal bonded complexes under thermal conditions, on extrusion of ammonia.

Results and discussion

Treatment of the parent amido complex [Ir(μ-NH₂)(cod)]₂ (**1**) with two molar equiv. of diphenylphosphane afforded the mixed bis(phosphido) amido-bridged diiridium complex

^aInstituto de Síntesis Química y Catálisis Homogénea ISQCH, Universidad de Zaragoza-CSIC, C/Pedro Cerbuna, 12, 50009 Zaragoza, Spain.

E-mail: mcasado@unizar.es, oro@unizar.es; Fax: +34 976 761 187;

Tel: +34 976 761 143

^bDepartamento de Química Física e Instituto de Biocomputación y Física de Sistemas Complejos (BIF), Universidad de Zaragoza, 50009 Zaragoza, Spain

^cCenter for Refining & Petrochemicals King Fahd University of Petroleum & Minerals, Dhahran, 31261, Saudi Arabia

† Dedicated to the memory of Professor María Pilar García Clemente.

‡ Electronic supplementary information (ESI) available: Additional experimental and full computational details (PDF). CCDC 951633–951635. For ESI and crystallographic data in CIF or other electronic format see DOI: 10.1039/c3dt52911h

[[1- κ -4,5- η^2 -C₈H₁₃Ir(μ -NH₂)(μ -PPH₂)₂Ir(1,2,5,6- η^4 -cod)] (3) (cod = 1,5-cyclooctadiene) in an excellent yield as a deep red, air-sensitive microcrystalline solid. Complex 3 can be formally described as the result of an exchange of an amido group by a phosphido ligand in 1 plus the net addition of diphenylphosphane to a postulated mixed phosphido/amido-bridged diiridium system. Accordingly, with this approach, other selected secondary phosphanes H-PR₂ reacted in a similar manner to 1, affording complexes [[1- κ -4,5- η^2 -C₈H₁₃Ir(μ -NH₂)(μ -PR₂)₂Ir(1,2,5,6- η^4 -cod)] (R = Cy (4), ⁱPr (5)) as red solids in acceptable yields, which were characterized in solution by multinuclear NMR techniques, including ¹H-¹⁵N HMQC spectroscopy and mass spectrometry.

In order to gain insight into the mechanism of the formation of 3–5, we monitored the reaction of 1 with diphenylphosphane at various temperatures by NMR techniques. We found that below –40 °C there is a clean and quantitative formation of new hydrido phosphido/amido diiridium species [(η^4 -cod)(H)Ir(μ -NH₂)(μ -PPH₂)₂Ir(η^4 -cod)] (2) along with release of one molar equiv. of ammonia. Above –10 °C, complex 2 is gradually transformed into 3 (Scheme 1).

Both dinuclear complexes 2 and 3 were fully characterized in solution by multinuclear NMR techniques and in the solid state by X-ray diffraction studies (see below). While deep-red crystals of 3 were obtained from concentrated solutions of the complex in toluene and hexane mixtures, the isolation and measurement of an orange monocrystal of 2 required careful manipulation at low temperatures (below –40 °C) throughout the process.

Fig. 1 and 2 show the molecular structures of complexes 2 and 3, both having dinuclear cores, with the metals bridged by two diphenylphosphido ligands located at opposite sides of the iridium–iridium axes, and an amido ligand. Although both dinuclear species share the same chemical composition, there are remarkable structural differences between them. While complex 2 displays a clearly non-bonding intermetallic separation (Ir1...Ir2 3.2928(3) Å), 3 shows a very short Ir–Ir bond (Ir1–Ir2 2.6795(3) Å), favoured by the flexibility of the phosphido and amido ligands in these dinuclear systems. This pliability is clearly seen in the central Ir₂P₂N cores. Differences in

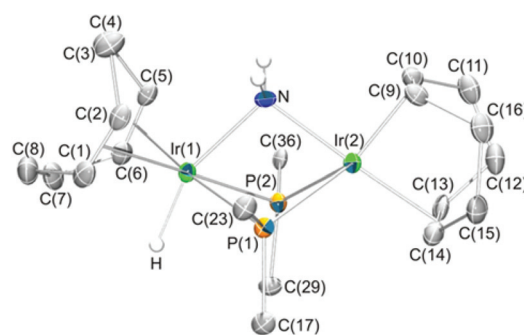


Fig. 1 Crystal structure of complex 2. Only hydrogen atoms for the hydride and the amido ligand have been shown, and the phenyl rings of the phosphanes have been omitted for clarity. Selected bond lengths [Å] and angles [°]: Ir(1)–P(1) 2.3764(10), Ir(1)–P(2) 2.3669(10), Ir(2)–P(1) 2.4190(10), Ir(2)–P(2) 2.3937(10), Ir(1)–N 2.175(3), Ir(2)–N 2.131(3), mean Ir–Ct 2.060(2), Ir(1)–H 1.608(19), P(1)–Ir(1)–P(2) 75.56(4), P(1)–Ir(2)–P(2) 74.28(3), P(1)–Ir(1)–N 72.87(10), P(2)–Ir(1)–N 75.32(10), P(1)–Ir(2)–N 72.73(10), P(2)–Ir(2)–N 75.53(10), P(1)–Ir(1)–Ct(2) 172.67(13), P(2)–Ir(1)–Ct(1) 177.25(11), P(1)–Ir(2)–Ct(3) 136.50(13), P(2)–Ir(2)–Ct(4) 106.21(13), N–Ir(2)–Ct(4) 177.64(16), N–Ir(1)–H 156.5(18). Ct(1), Ct(2), Ct(3) and Ct(4) represent the midpoints of the olefinic C(1)–C(2), C(5)–C(6), C(9)–C(10) and C(13)–C(14) bonds, respectively.

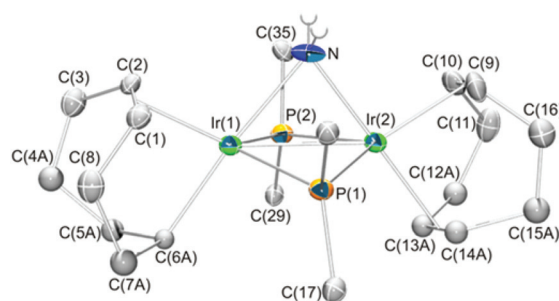
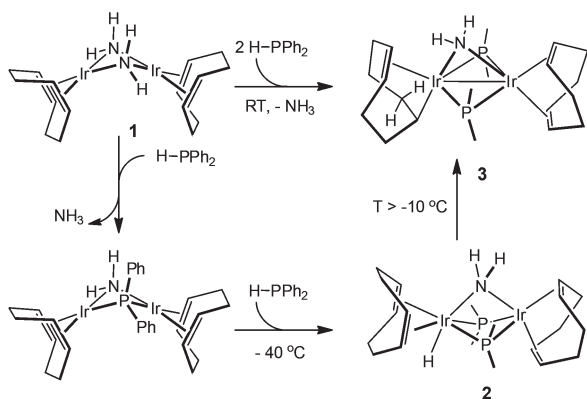


Fig. 2 Crystal structure of complex 3. Only hydrogen atoms for the hydride and the amido ligand have been shown, and the phenyl rings of the phosphanes have been omitted for clarity. Selected bond lengths [Å] and angles [°]: Ir(1)–P(1) 2.3321(15), Ir(2)–P(1) 2.3459(15), Ir(1)–P(2) 2.3067(15), Ir(2)–P(2) 2.3841(15), Ir(1)–N 2.180(5), Ir(2)–N 2.125(5), Ir(1)–Ct(1) 1.993(6), Ir(2)–Ct(2) 1.993(6), Ir(1)–C(6A) 2.098(9), Ir(2)–Ct(3) 2.089(9), Ir(1)–Ir(2) 2.6795(3), P(1)–Ir(1)–P(2) 109.59(5), P(1)–Ir(2)–P(2) 106.51(5), P(1)–Ir(1)–N 74.86(15), P(1)–Ir(2)–N 70.58(14), P(1)–Ir(1)–Ct(1) 119.0(2), P(1)–Ir(2)–Ct(2) 131.8(2), P(1)–Ir(2)–Ct(3) 101.8(2), P(2)–Ir(1)–N 76.05(14), P(2)–Ir(2)–N 75.42(16), P(2)–Ir(1)–C(6A) 102.6(3), P(2)–Ir(2)–Ct(3) 106.4(2), N–Ir(1)–C(6A) 174.8(3), N–Ir(2)–Ct(3) 177.2(3), Ct(1)–Ir(1)–C(6A) 83.1(3), Ct(2)–Ir(2)–Ct(3) 83.7(3). Ct(1), Ct(2) and Ct(3) represent the midpoints of the olefinic C(1)–C(2), C(9)–C(10) and C(13A)–C(14A) bonds, respectively.



Scheme 1 Formation of complexes 2 and 3.

the coordination of the diphenylphosphido bridges not only affect its asymmetry (more pronounced in 3), but also the bond length (longer in 2) and angle values (mean P–Ir–P angle values: 74.92(2) and 108.05(3)° in 2 and 3, respectively). The two iridium and the two phosphorus atoms display a butterfly disposition, with a [P1Ir1P2]–[P1Ir2P2] dihedral angle of 59.51(3)° in 2 and 26.41(5)° in 3. The metal coordination geometries reflect the distinct formal oxidation states: thus, the Ir1 atom shows a distorted octahedral environment,

surrounded by a cod ligand, two bridging phosphorus atoms and one nitrogen atom, and the hydride, *trans* to the latter, while Ir2 exhibits a trigonal bipyramid geometry, with the phosphorus atoms and one olefinic bond of the cod ligand defining the trigonal plane. This situation differs from that shown in 3, in which both Ir geometries can be described as severely distorted octahedra with the two phosphorus atoms in apical positions. Both complexes also differ in the coordination of the carbocyclic ligands; while in 2 the diolefins are coordinated in their usual $\eta^4\text{-C}=\text{C}$ mode, but are rotated 90° with each other (due to the presence of the hydride ligand), in 3 the initial diolefin attached to Ir1 has become a cyclooctenyl ligand $\kappa\text{-C}$ metallated *trans* to the amido nitrogen atom and $\eta^2\text{-C}=\text{C}$ coordinated to iridium.

The multinuclear NMR spectra of intermediate 2 showed some peculiarities derived from a non-rigidity phenomenon operative within the diiridium system. More precisely, while the cod attached to the octahedral iridium atom Ir1 in 2 gave two signals both in the ^1H and $^{13}\text{C}\{^1\text{H}\}$ NMR spectra, as expected for the C_s symmetry observed in the solid state, the other cod molecule was found to undergo a fluxional motion, more likely described as a propeller-like rotation that makes both =CH and CH₂ protons and carbons of this carbocyclic ligand chemically equivalent at all temperatures, respectively. The VT NMR spectra in CD₂Cl₂ did not show any decoalescence at the lowest temperature available (−90 °C), indicating an unexpected low barrier for cod rotation. Its origin is most likely related to the intrinsic stereochemical non-rigidity usually associated with pentacoordinated low-valent late metal complexes.¹² On the other hand, the hydrido ligand was located at δ −13.28 ppm as a triplet, and showed a strong NOE effect with the =CH protons pointing downwards of the amido ligand at Ir1 (those attached to C1 and C6 in Fig. 1), and the $^{31}\text{P}\{^1\text{H}\}$ NMR spectrum reflected the C_s symmetry observed in the molecular structure of 2, since it showed a sole signal at −108.1 ppm. The equivalent amido protons emerged as a broad triplet at high field ($\delta(^1\text{H})$ −0.71 ppm; $\delta(^{15}\text{N})$ −174.6 ppm).

The NMR spectra of complex 3 reflected the lack of symmetry observed in the molecular structure at various temperatures. A set of 2D NMR experiments allowed unambiguously assigning each resonance in both carbocyclic olefins (see ESI†). More specifically, the metallated Ir–CH group was observed at 2.55 and 9.2 ppm in the ^1H and $^{13}\text{C}\{^1\text{H}\}$ NMR spectra, respectively, while six well-separated resonances were clearly identified for each =CH carbon of both carbocyclic molecules. It is worth mentioning the unusual shift to low field and multiplicity observed for the methylenic carbon (labelled as C5A in Fig. 2) in the $^{13}\text{C}\{^1\text{H}\}$ NMR spectra (δ 50.0, $^3J_{\text{C-P}} = 9$ Hz), which corresponds precisely to the =CH carbon initially coordinated to iridium in complex 2. These characteristic resonances were reflected in the related complexes 4 and 5, which showed their respective methylenic carbons at 51.2 and 50.5 ppm in their $^{13}\text{C}\{^1\text{H}\}$ NMR spectra, respectively. A significant feature of complexes 3–5 was the presence of signals at high field that corresponded to the bridging amido protons.

While complex 2 gave two well-resolved multiplets centred at −3.61 ppm ($\delta(^{15}\text{N})$ −100.3 ppm) at room temperature, those for 4 and 5 were observed as broad multiplets at −3.71 and −3.83 ppm at −40 °C, respectively, which correlated with nitrogen resonances at −103.2 (4) and −104.6 (5) in their $^{15}\text{N}\text{-}^1\text{H}$ HMBC spectra.

The $^{31}\text{P}\{^1\text{H}\}$ NMR spectra of 4–6 were virtually identical, all of them showing an AB pattern at very low fields ($\delta(^{31}\text{P})$: 91.2 (3); 113.3 (4); 125.6 (5)). The marked difference in chemical shift for the phosphane bridging ligands in 2 and 3 ($\Delta\delta = 199$ Hz) should have its origin on the oxidation states of the metals (and therefore on their geometry) in both complexes.¹³ From this point of view, complex 2 can be described as a mixed-valence species Ir^{III}/Ir^I (where the Ir^{III} centre is labelled as Ir1 in Fig. 1) without metal–metal bonds. In contrast, complex 3 displays a short iridium–iridium bond, a situation that could be formally associated with an Ir^{II}–Ir^{II} metal–metal bonded system or an Ir^{III} ← Ir^I dinuclear complex in which the Ir^I atom displays a dative bond to Ir^{III} (Ir2 and Ir1 respectively, in Fig. 2).¹⁴ A geometrical analysis of 3 reveals general trends similar to those observed in 2: the Ir2–P bond distances are longer than Ir1–P ones, while the Ir2–N bond length is shorter than Ir1–N, a situation that seems to be in favour of the possible existence of an intermetallic dative bond connecting the two metals and reducing significantly their electronic differences. An analysis of the NBO atomic charges of DFT calculated structures 2 and 3 has been performed in order to gain insight into the oxidation state of Ir centers. In complex 2, a difference of 0.2374 electron can be observed between the Ir1 ($q_{\text{Ir1}} = -0.6219$) and Ir2 ($q_{\text{Ir2}} = -0.3845$) centers. On the other hand, in complex 3 both Ir centers present very similar charges $q_{\text{Ir1}} = -0.4570$ and $q_{\text{Ir2}} = -0.4268$. These results suggest a different electronic structure between Ir centers in complex 2 while a more similar electronic environment is expected in complex 3. It is interesting to point out that the Ir₂P₂N core is flexible enough to allow the structural changes that encompass the transformation 2 → 3, which are resembled in the geometry of the iridium centers, always held in close proximity by the triply-bridged system.

Remarkably, complex 2 results from a formal oxidative addition of a P–H bond to a low-valent metal complex.¹⁵ The overall formation of 2 implies two P–H bond activation processes of different nature: (i) a heterolytic split leads to an NH₂/PPh₂ exchange, and (ii) an iridium atom from the resulting mixed amido/phosphido species induces a homolytic scission of the P–H bond of a second molecule of diphenylphosphane giving formally a one-centre net *cis* addition of H–PPh₂. The former process should lead to a dinuclear intermediate [(cod)Ir(μ-NH₂)(μ-PPh₂)Ir(cod)] (Scheme 1) as supported by theoretical calculations (see ESI†), with ammonia being formed in the process; as a matter of fact, the rhodium analogue [Rh₂(μ-NH₂)(μ-PPh₂)(cod)₂] was readily observed *in situ* by NMR spectroscopy on the addition of H–PPh₂ to the rhodium bis(amido) complex [{Rh(μ-NH₂)(cod)}₂], along with the formation of the known bis(phosphido) species [{Rh(μ-PPh₂)(cod)}₂]¹⁶ and free ammonia (see ESI†). In complex 2 the

hydrido ligand is coplanar with one of the C=C double bonds of the neighbouring coordinated cod, a situation that usually leads to a facile hydride transfer from the metal to the olefin, affording in the present case unsaturated species **3**, a process that has already been observed for some mononuclear late metal systems.¹⁷

The fate of the protons attached to phosphorus in diphenylphosphane on interaction with **1** was clearly determined by making use of isotope labelling techniques. The reaction of **1** with two molar equiv. of D-PPh₂ was followed using ²H NMR spectroscopy, and this allowed observing the release of the ammonia isotopomer ND₂H (δ -0.32 ppm) and a sole signal at δ 1.94 ppm, which specifically corresponded to one of the protons attached at C5A (Scheme 2, **3-d**₁). No deuterium scrambling was observed in solutions of **3-d**₁ for a prolonged time at room temperature. The net incorporation of deuterium at that methylenic carbon was reflected both in the multiplicity of the phosphorus resonance by coupling with deuterium and in an upfield shift of 0.2 ppm in the ³¹P{¹H} NMR spectrum of **3-d**₁. In turn, treatment of the *N*-deuterated complex [{Ir(μ -ND₂)(cod)}₂] with diphenylphosphane allowed observing by ²H spectroscopy the amido deuterium atoms as the only iridium species (δ -3.6 ppm), along with release of the ND₂H isotopomer (δ -0.21 ppm), an observation that evidenced that protons of one of the amido ligands do not participate in the formation of **2** and **3**.

Some observations made from the above experiments allowed us to observe H/D exchange processes promoted by complex **3** in solution at room temperature. As a matter of fact, treatment of **3** with D-PPh₂ (δ (³¹P) -42.6 ppm) showed, after ten minutes, the formation of free H-PPh₂ (δ (³¹P) -41.3 ppm) and the net incorporation of deuterium at C5A as a consequence of an intermolecular H/D exchange. Interestingly, ammonia was also found to participate in such intermolecular exchange events. When a solution of **3** in toluene was treated with ND₃ at atmospheric pressure in a Young NMR tube, we observed selective H/D exchange and net incorporation of deuterium specifically at the C5A carbon within 30 minutes along with concomitant formation of ND₂H, as confirmed by ²H, ¹H and ³¹P{¹H} NMR spectroscopy. In the same lines, when D₂O or CD₃OD was used as a deuterated reagent in

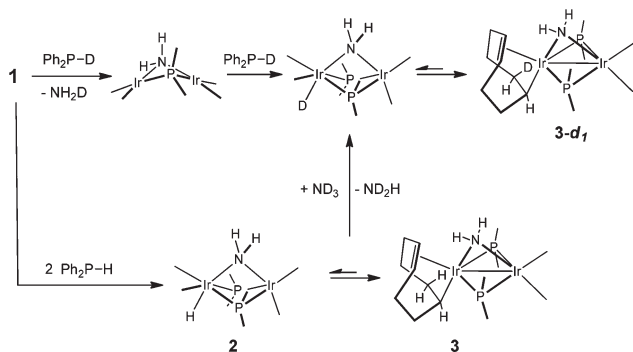
conjunction with complex **3**, slow incorporation of deuterium at that methylenic carbon was observed in the ²H NMR spectra.

These H/D exchange processes could in principle be explained taking into consideration the microreversibility status that may be established between complexes **2** and **3**.¹⁸ Although we have not been able to observe complex **2** on dissolution of complex **3** at low temperatures by NMR techniques, species **2** should be present in the medium albeit in undetectable concentrations. From this perspective, it may be argued that the H/D exchange occurs actually not on **3**, but instead on complex **2** specifically at the hydrido site. In this context, there are some reports dealing with hydrogen exchange processes at hydrido late metal complexes with weak proton donors that revealed that protonation at the hydrido moiety does indeed lead to hydrogen exchange.¹⁹ From this perspective, we propose that it is the mixed-valence hydrido complex **2** that is actually responsible for the H/D exchange processes observed experimentally. In this way, the hydrido ligand in **2** may undergo H/D exchange with protic deuterated reagents forming the deuterido analogue [(η^4 -cod)(D)Ir(μ -NH₂)-(μ -PPh₂)₂Ir(η^4 -cod)], which then experiences a transfer process to the coordinated cod molecule selectively to the C5A carbon affording **3-d**₁ as the only observable product (Scheme 2).

Indirect evidence of the microreversibility status established between species **2** and **3** (and therefore of the presence of complex **2** in solution) came from the observed catalytic activity in olefin isomerization. For instance, when solutions of **3** in [D₆]benzene were treated with 100-fold excess of 2-allylphenol at room temperature for 24 h, quantitative isomerization to a 40 : 60 mixture of the *Z* and *E* isomers, respectively, was observed. Allyl benzene required 60 °C to isomerize to a 35 : 65 mixture of the *Z* and *E* isomers in 75%. Since catalytic isomerization of olefins is often promoted by hydrido metal complexes,²⁰ it is reasonable to believe that the actual isomerization catalyst should be the hydrido complex **2**, which should be present in equilibrium with **3** to a certain degree, as stated above.

On the other hand, heating toluene solutions of **3** in a Young NMR pressure tube at 120 °C allowed observing conversion to the known bis(phosphido) complex [{Ir(μ -PPh₂)(cod)}₂]¹⁶ after 12 h, along with released ammonia. Full conversion of the related complexes **4**–**5** to the corresponding novel phosphido-bridged derivatives [{Ir(μ -PR₂)(cod)}₂] (R = Cy (**6**), ⁱPr (**7**)) was achieved under milder conditions (see ESI[†]). As a matter of fact, the ⁱPr complex **5** slowly transformed at room temperature for 24 hours in toluene solutions to the corresponding phosphido-bridged species **7**.

Dinuclear phosphido complex **6** displayed two distinct signals for the =CH fragments from different cod molecules both in the ¹H and ¹³C{¹H} NMR spectra C_{2v} symmetry, a situation that indicated the selective formation of one of the three possible isomers, specifically that containing a square-planar iridium centre (16 e⁻) and a tetrahedral iridium (18 e⁻) connected by a metal–metal bond. The ³¹P{¹H} NMR singlet observed at δ 26.0 ppm supported this proposal, since it



Scheme 2 Deuterium labelling studies carried out on complex **1**.

is comparable to other structurally related dinuclear bis-(phosphido) late metal complexes found in the literature.²¹ In contrast, complex **7** was isolated as a 3 : 1 mixture of isomers. The most abundant one showed equivalent =CH cod fragments both in the ¹H and the ¹³C{¹H} NMR spectra and a significant signal at δ 230.0 ppm in the ³¹P{¹H} NMR spectrum, quite far from the resonance observed for the second isomer (δ 39.0 ppm). The low-field chemical shift observed for the major isomer nicely fits those observed in some related complexes which contain both metals around tetrahedral geometries; furthermore, it also fits the C_{2h} symmetry observed. On the other hand, the minor isomer corresponded to the square-planar-tetrahedral species: the pattern of the cod resonances was virtually similar to that shown by **6**, displaying a C_{2v} symmetry.

X-ray quality crystals of derivative **7** were obtained and subjected to an X-ray diffraction analysis. Fig. 3 shows the molecular structure of **7**, together with main bond lengths and angles. Complex **7** is dinuclear, with two phosphido ligands bridging both metals, and corresponds to the major C_{2h} isomer. The central Ir₂P₂ core, very different from those observed in **2** and **3**, is almost planar; the dihedral angle between the [P1Ir1P2] and [P1Ir2P2] planes is 0.08(3)°. Moreover, Ir–P bond lengths are significantly shorter than those previously reported for these amido-bridged complexes. As expected from other late metal phosphido-bridged systems, both metals display a strong intermetallic interaction illustrated by a very short Ir–Ir distance (Ir1=Ir2 2.60679(18) Å). This short intermetallic distance, which is shorter than that observed in [{Ir(μ-PCy₂)(Cl)(CO)(PEt₃)₂}] (Ir–Ir 2.762(1) Å), formally an Ir^{II}–Ir^{II} single metal–metal bonded complex,²² matches well with those found in structurally related phosphido-bridged diiridium complexes, such as in [{Ir(CO)(PPh₃)-

(μ-PPh₂)₂] (2.551(1) Å),²³ [{Ir(CO)₂(μ-P^tBu₂)₂}]₂ (2.545(1) Å),²⁴ [{Ir(PEt₃)₂(μ-η^{-2,4}-dimethylphosphapentadienyl)]₂ (2.587(1) Å),^{25a} and [{Ir(PEt₃)₂(μ-η⁻¹-phosphapentadienyl)]₂ (2.576(1) Å),^{25b} all of them examples considered to feature Ir=Ir double bonds. Under this consideration, the electron count of 18 e⁻ for each iridium in **7** is reflected in the tetrahedral geometry around both metals.²⁶

The thermal reactions that lead to phosphido-bridged complexes are sound examples of reductive elimination of ammonia, a rare phenomenon (the reverse process of oxidative addition of ammonia) seldom observed in late metal complexes.^{27,10b} In the mixed amido-phosphido bridged complexes, the NH₂ fragment is tightly bound to both metals, as observed both experimentally and theoretically specifically in complex **3** (see below), remaining unaltered throughout the sequential transformation: **1** → **2** → **3**. Along this manifold, the reductive elimination of ammonia should take place from hydrido complex **2**. On the other hand, the temperature required to achieve elimination of ammonia from complex **2** has been found to be higher than that needed for derivatives **4** and **5** (PⁱPr₂ and PCy₂ phosphido bridges, respectively), indicating that basicity injected in the bimetallic system by the phosphido ligands facilitates the NH₃ reductive elimination process.

The reactions shown in this work have been examined by DFT calculations at the B3LYP level. Hence, the reaction energy profile for the transformation of **1** (structure **A**) into **2** (structure **C**) and **3** (structure **D**) is presented in Fig. 4. The replacement of the amido bridge in **A** by the phosphido-bridge in **B** on addition of diphenylphosphane and release of ammonia is an exothermic reaction (−7.1 kcal mol⁻¹) with an energy barrier of 8.3 kcal mol⁻¹. The energetic profile of this process is shown in the ESI (Fig. S1†) and it takes place *via* phosphide coordination to the metal, followed by amido-bridge decoordination from one metallic centre and hydrogen transfer from the phosphide group to the lone pair of the NH₂ moiety. Addition of a second phosphane molecule to **B** follows a different process as shown in Fig. 4. The oxidative addition of the P–H bond to the Ir occurs through the transition structure **TS_{B/C}** with an activation barrier of 21.4 kcal mol⁻¹. The lone pair of the Ir–PPh₂ moiety can coordinate to the other Ir centre yielding complex **C**, which corresponds to complex **2**. The migration of the hydride to the cod ligand takes place *via* the transition structure **TS_{C/D}** with an activation energy of 21.5 kcal mol⁻¹, yielding structure **D** (corresponding to complex **3**).

The energetic profile for the reductive elimination of ammonia from **2** to yield complex **6** is presented in Fig. 5. The energy required to de-coordinate the amido-bridge from one metal yielding the **int4** structure is 13.1 kcal mol⁻¹ and reductive elimination of NH₃ occurs through the **TS_{C/E}** structure. The energetic barrier for this process relative to the resting state **D** is 39.2 kcal mol⁻¹ and therefore high temperatures are needed (it is experimentally observed at 120 °C). The outcome of this process is the ammonia adduct of the phosphido-bridged complex **E**. Geometry optimization of the complex **E**⋯NH₃ on removal of ammonia leads to the observed complex

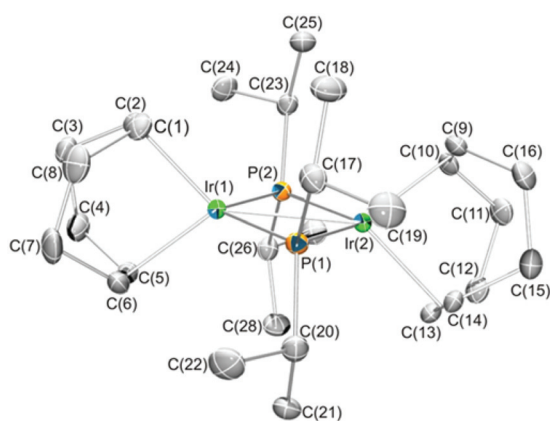


Fig. 3 Crystal structure of complex **7**. Selected bond lengths [Å] and angles [°]: Ir(1)=Ir(2) 2.60679(18), Ir(1)–P(1) 2.2808(7), Ir(1)–P(2) 2.2783(7), Ir(2)–P(1) 2.2989(8), Ir(2)–P(2) 2.2994(7), mean Ir–Ct 2.061(1), P(1)–Ir(1)–P(2) 111.30(3), P(1)–Ir(2)–P(2) 109.88(2), P(1)–Ir(1)–Ct(1) 117.72(8), P(1)–Ir(2)–Ct(3) 128.46(8), P(2)–Ir(1)–Ct(2) 116.56(9), P(2)–Ir(2)–Ct(4) 128.77(8), Ct(1)–Ir(1)–Ct(2) 83.63(11), Ct(3)–Ir(2)–Ct(4) 83.83(11). Ct(1), Ct(2), Ct(3) and Ct(4) represent the midpoints of the olefinic C(1)–C(2), C(5)–C(6), C(9)–C(10) and C(13)–C(14) bonds, respectively.

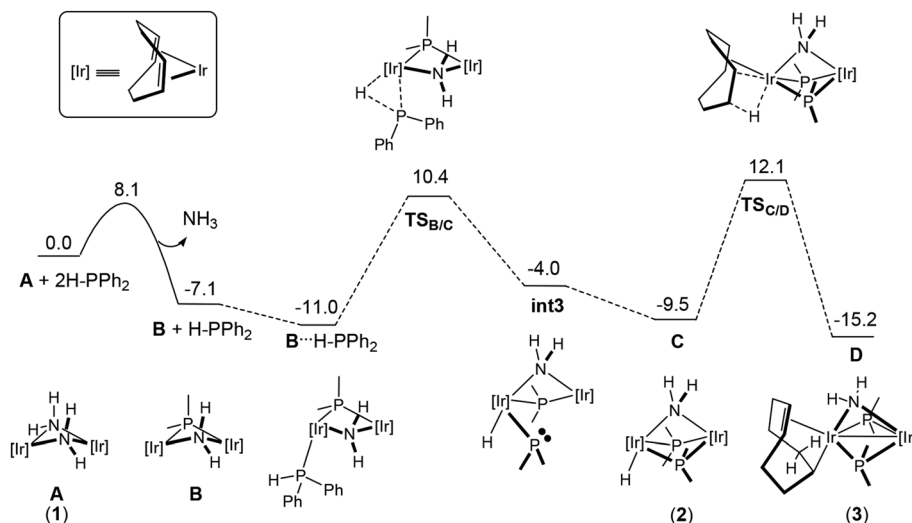


Fig. 4 Computed DFT potential-energy profile (ΔE in kcal mol⁻¹) for the formation of complex **3** from **1** and two molecules of diphenylphosphane.

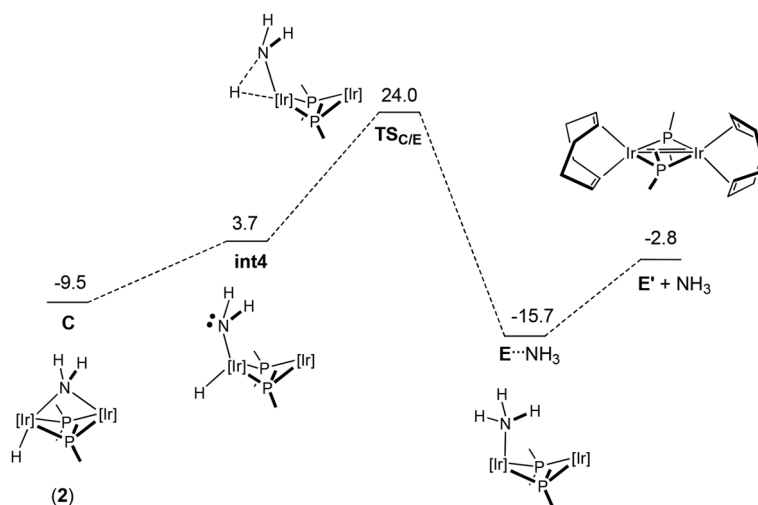


Fig. 5 Computed DFT potential-energy profile (ΔE in kcal mol⁻¹) for the reductive elimination of ammonia from complex **2**.

E' (corresponding to the known complex $[\{\text{Ir}(\mu\text{-PPh}_2)(\text{cod})\}_2]$). In summary, this DFT investigation shows that the transformation $1 \rightarrow 2 \rightarrow 3$ is thermodynamically favored with activation barriers affordable at low temperatures, while the reductive elimination of NH_3 to yield **6** can only take place at high temperatures.

Conclusions

We have shown a parent amido diiridium complex able to activate the P–H bond of a variety of secondary phosphanes under mild conditions, rendering unusual triply-bridged amido/phosphido species quite sensitive to temperature. It is noteworthy that throughout the chemical transformations described within the dinuclear system, only one iridium atom seems to be involved both in the activation of P–H bonds (and the subsequent olefin migratory insertion to a Ir–H bond) and

in the formation of ammonia by undergoing respectively elementary oxidative addition (P–H) and reductive elimination (N–H) processes, where this metal experiences variations in its oxidation state. We believe that this chemistry is partly fuelled by the presence of a neighboring iridium basic center, which, due to the high flexibility of the triply-bridged ligand system, is indeed able to approach the other metal establishing an intermetallic bond that helps in stabilizing these species.

Experimental

All manipulations were performed under a dry argon atmosphere using Schlenk-tube techniques. Solvents were obtained from a solvent purification system (Innovative Technologies) or were dried by standard procedures and distilled under argon prior to use. HPPH_2 , HPCy_2 and HPiPr_2 were purchased from Aldrich and gaseous NH_3 and ND_3 were commercially obtained

and used without further purification. D-PPh₂²⁸ and complexes **1** and [$\{\text{Rh}(\mu\text{-NH}_2)(\text{cod})\}_2$] were prepared as previously described in the literature.^{8a} All the other chemicals used in this work have been purchased from Aldrich Chemicals and used as received. Carbon, hydrogen and nitrogen analyses were performed using a Perkin-Elmer 2400 CHNS/O microanalyzer. Mass spectra were recorded on a VG Autospec double-focusing mass spectrometer operating in the FAB⁺ mode. Ions were produced with the standard Cs⁺ gun at ca. 30 kV; 3-nitrobenzyl alcohol (NBA) was used as a matrix. ESI-MS were recorded on a Bruker Micro-Tof-Q by using sodium formate as a reference. ¹H, ³¹P{¹H} and ¹³C{¹H} NMR spectra were recorded on a Varian UNITY, Bruker ARX 300, and Bruker Avance 400 spectrometers operating at 299.95, 121.42 and 75.47 MHz, 300.13, 121.49 and 75.47 MHz, and 400.13, 161.99 and 100.00 MHz, respectively. Chemical shifts are reported in ppm and referenced to Me₄Si using the residual signal of the deuterated solvent (¹H and ¹³C), H₃PO₄ as an external reference (³¹P) and liquid NH₃ (¹H-¹⁵N HMQC).

[(η^4 -cod)(H)Ir(μ -NH₂)(μ -PPh₂)₂Ir(η^4 -cod)] (2)

Pure diphenylphosphane (47 mg, 44 μ L, 0.25 mmol) was slowly added *via* a microsyringe to a pre-cooled solution of **1** (80 mg, 0.13 mmol) in dichloromethane (8 mL) at -50 °C, layered with cold hexanes, and then the mixture was left for 5 days at -38 °C. A small crop of orange crystals identified as complex **2** was separated very carefully, and a mono-crystal was subjected to X-ray analysis. The *in situ* ¹H NMR monitoring of the reaction of diphenylphosphane with **1** under these conditions allowed observing quantitative formation of complex **2** after 10 minutes. ¹H NMR (400 MHz, CD₂Cl₂, -50 °C): δ 7.86 (m, 4H, H^o), 7.61 (m, 4H, H^o), 7.31 (m, 4H, H^m), 7.24 (m, 2H, H^m), 7.05 (m, 6H, H^o + H^m) (PPh₂), 4.39 (m, 2H, =CH), 3.11 (m, 4H, =CH), 2.42 (m, 8H, =CH + CH₂), 2.08 (m, 2H), 1.87 (m, 6H), 1.63 (m, 2H) (CH₂) (cod), -0.71 (t, 2H, ³J_{H-P} = 15.9 Hz, NH₂), -13.28 (br t, 1H, ²J_{H-P} = 15.0 Hz, Ir-H). ³¹P{¹H} NMR (162 MHz, CD₂Cl₂, -50 °C): δ -108.1 (s). ¹³C{¹H} RMN (100 MHz, CD₂Cl₂, -50 °C): δ 136.1 (s, C^o), 135.8 (d, ¹J_{C-P} = 20 Hz, C^{ipso}), 135.7 (d, ¹J_{C-P} = 20 Hz, C^{ipso}), 133.8 (s, C^o), 127.7 (s, C^m), 127.3 (s, C^m), 126.9 (s, C^p), 126.1 (s, C^p) (PPh₂), 83.6, 75.6, 54.8 (all s, =CH), 34.0, 34.2, 28.4 (all s, CH₂) (cod). ¹⁵N-¹H HMQC (40 MHz, d₈-toluene, -40 °C): δ -174.6.

[(1- κ -4,5- η^2 -C₈H₁₃)Ir(μ -NH₂)(μ -PPh₂)₂Ir(1,2,5,6- η^4 -cod)] (3)

Pure diphenylphosphane (0.09 g, 82 μ L, 0.47 mmol) was slowly added *via* a syringe to a red solution of **1** (0.15 g, 0.24 mmol) in toluene (8 mL), giving rise to a dark red solution which was stirred for 45 min. The solvent was then removed *via* cannula and the remaining red solid was washed repeatedly with hexanes and then dried under vacuum. Yield: 0.21 g (89%). ¹H NMR (300 MHz, C₆D₆): δ 8.24 (m, 4H, H^o), 7.63 (m, 2H, H^o), 7.27-6.73 (m, 14H, H^o + H^m + H^p) (PPh₂), 3.89 (m, 1H, =CH¹), 3.65 (m, 1H, =CH²), 3.58 (m, 1H, =CH¹³), 3.51 (m, 1H, =CH¹⁴), 3.37 (m, 1H, H⁸), 3.14 (m, 1H, =CH¹⁰), 2.83 (m, 1H, H⁸), 2.75 (m, 1H, H¹⁵), 2.68 (m, 1H, H¹⁵) (CH₂), 2.55 (m, 1H, Ir-CH⁶),

2.45 (m, 1H, =CH⁹), 2.40 (m, 1H, H⁷), 2.34 (m, 2H, H⁷ + H³), 2.26 (m, 1H, H¹¹), 2.05 (m, 1H, H¹¹), 1.97 (m, 1H, H¹²), 1.93 (m, 1H, H¹⁶), 1.79 (m, 2H, H⁵ + H⁵), 1.73 (m, 1H, H¹²), 1.67 (m, 1H, H³), 1.54 (m, 1H, H¹⁶), 1.44 (m, 2H, H⁴ + H⁴) (CH₂) (cod), -3.45 (m, 1H), -3.77 (m, 1H) (NH₂). ³¹P{¹H} NMR (121 MHz, C₆D₆): δ 91.2 (AB system). ¹³C{¹H} RMN (75 MHz, C₆D₆): δ 138.6 (m, C^{ipso}), 136.4, 132.7, 131.6 (m, C^o), 129.7 (m, C^{ipso}), 128.9 (d, ³J_{C-P} = 5 Hz, C^m), 128.1, 127.9, 127.8 (C^m + C^p) (PPh₂), 78.5 (s, =C¹⁴H), 75.3 (s, =C¹³H), 56.7 (d, ²J_{C-P} = 10 Hz, =C¹⁰H), 56.0 (dd, ²J_{C-P} = 14 Hz, ³J_{C-P} = 3 Hz, =C⁹H), 54.3 (dd, ²J_{C-P} = 15 Hz, ³J_{C-P} = 4 Hz, C²), 50.0 (t, ²J_{C-P} = 9 Hz, C⁵), 42.2 (d, ²J_{C-P} = 12 Hz, C¹), 38.3 (s, C¹⁵), 37.1 (s, C⁴), 37.0 (s, C¹¹), 33.0 (s, C¹⁶), 30.6 (s, C³), 30.1 (s, C⁷), 29.9 (s, C⁸), 29.6 (s, C¹²), 9.2 (t, ²J_{C-P} = 3 Hz, Ir-C⁶). ¹⁵N-¹H HMQC (40 MHz, d₈-toluene, -40 °C): δ -100.3. MS (ESI⁺): *m/z* 987.0 [M⁺ - H], 971.2 [M⁺ - NH₂]. Anal. Calcd (%) for C₄₀H₄₇Ir₂NP₂ (988.19): C 48.62, H 4.79, N 1.42; found: C 48.03, H 4.75, N 1.71.

[(1- κ -4,5- η^2 -C₈H₁₃)Ir(μ -NH₂)(μ -PCy₂)₂Ir(1,2,5,6- η^4 -cod)] (4)

Pure dicyclohexylphosphane (0.09 g, 0.47 mmol) was slowly added *via* a syringe to a solution of **1** (0.15 g, 0.24 mmol) in toluene (6 mL), giving rise to a dark red mixture which was stirred for 1 hour. The solvent was then removed under vacuum leaving an oil that was subsequently washed with hexanes, affording a red solid which was isolated *via* cannula and dried under vacuum (0.22 g, 92%). ¹H NMR (400 MHz, d₈-toluene, -40 °C): δ 4.26 (m, 1H, =CH), 3.64 (m, 2H, =CH + CH₂), 3.21 (m, 1H, =CH), 3.12 (m, 1H, =CH), 2.86 (m, 3H, CH₂), 2.80 (m, 4H, Ir-CH + CH₂), 2.54 (m, 12H), 2.30 (m, 6H), 2.02 (m, 12H), 1.76 (m, 12H), 1.35 (m, 12H) (CH₂ cod + PCy₂), -3.71 (br m, 2H, NH₂). ³¹P{¹H} NMR (121 MHz, d₈-toluene, -40 °C): δ 113.3 (AB system). ¹³C{¹H} RMN (75 MHz, d₈-toluene, -40 °C): δ 64.8 (s, =CH), 62.8 (s, =CH), 51.0 (m, CH₂), 48.0 (m, =CH), 47.0 (m, =CH), 46.9 (m, =CH), 41.2 (s, CH₂) (cod), 40.8, 40.3 (m, C^{ipso} PCy₂), 48.9, 35.6 (m, =CH cod), 32.2, 31.9, 31.5, 31.2, 29.6, 28.4, 28.2, 27.6, 27.0, 26.5 (set of s; CH₂ cod + PCy₂), 3.0 (s, Ir-CH). ¹⁵N-¹H HMQC (40 MHz, d₈-toluene, -40 °C): δ -103.2. MS (micro-TOF): *m/z* 995.4057 [M⁺ - NH₂]. Anal. Calcd (%) for C₄₀H₇₁Ir₂NP₂: C 47.46, H 7.07, N 1.38; found: C 47.03, H 4.75, N 1.71.

[(1- κ -4,5- η^2 -C₈H₁₃)Ir(μ -NH₂)(μ -PⁱPr)₂Ir(1,2,5,6- η^4 -cod)] (5)

A solution of diisopropylphosphane (10% in hexane, 0.81 g, 0.67 mmol) was slowly added *via* a syringe to a solution of **1** (0.20 g, 0.33 mmol) in toluene (8 mL), giving rise to a dark red solution. On stirring the mixture for 1 hour, the solvent was dried under vacuum and the oil obtained was washed with hexane, giving rise to a dark suspension. The solvent was removed *via* cannula and the solid was washed repeatedly with hexanes and then dried under vacuum (0.13 g, 41%). ¹H NMR (300 MHz, d₈-toluene, -40 °C): δ 3.84 (m, 1H, =CH), 3.74 (m, 1H, CH₂), 3.38 (m, 1H, =CH), 3.24 (m, 1H, =CH), 3.04 (m, 1H, =CH), 2.70 (m, 4H, CHⁱPr + CH₂ + =CH cod), 2.54 (m, 1H, Ir-CH), 2.43 (m, 4H, =CH + CH₂), 2.33 (m, 2H, CH₂), 2.15 (m, 4H, CH₂), 1.95 (m, 2H, CH₂), 1.76 (m, 2H, CH₂), 1.56 (m, 8H, CH₂ cod + CH, CH₃ⁱPr), 1.45 (m, 9H), 1.37 (m, 3H),

1.22 (m, 3H), 1.01 (m, 3H), 0.79 (m, 3H) (CH₃ⁱPr), -3.83 (br m, 2H, NH₂). ³¹P{¹H} NMR (100 MHz, d₈-toluene, -40 °C): δ 125.6 (AB system). ¹³C{¹H} RMN (75 MHz, d₈-toluene, -40 °C): δ = 64.6 (s, =CH), 62.2 (s, =CH), 51.3 (m, =CH), 50.5 (t, ²J_{C-P} = 8 Hz, CH₂), 48.2 (d, ²J_{C-P} = 24 Hz, =CH), 47.4 (d, ²J_{C-P} = 21 Hz, =CH), 41.7 (m, CH₂), 37.4 (m, CH₂ cod), 35.2 (d, ²J_{C-P} = 15 Hz, =CH), 31.5 (s, CH₂), 30.0 (s, CH₂) (cod), 28.9, 27.9, 24.7, 24.0 (m, CHⁱPr), 22.9, 21.6, 21.5, 21.0 (s, CH₃ⁱPr), 2.9 (s, Ir-C). ¹⁵N-¹H HMQC (40 MHz, d₈-toluene, -40 °C): δ -104.6. MS (micro-TOF⁺): *m/z* 835.2822 (M⁺ - NH₂).

[{Ir(μ-PCy₂)(cod)}₂] (6)

A Young NMR tube was charged with 4 (15 mg), dissolved in [D₈]toluene (0.4 mL) and then sealed under argon. On heating the mixture at 80 °C for 3 hours, complete conversion to 6 was achieved. ¹H NMR (300 MHz, C₆D₆): δ 4.17 (m, 4H), 3.88 (m, 4H) (=CH cod), 2.31 (m, 4H), 2.17 (m, 4H) (CH₂ cod), 2.00 (m, 12H, CH₂ cod + C^m Cy), 1.65 (m, 12H, CH₂ cod + C^o Cy), 1.35 (m, 4H, C^{ipso} Cy), 1.04 (m, 4H, C^p Cy). ³¹P{¹H} NMR (121 MHz, C₆D₆): δ 26.0 (s). ¹³C{¹H} RMN (75 MHz, C₆D₆): δ 74.9 (d, ²J_{C-P} = 12 Hz), 54.6 (s) (=CH cod), 38.8 (d, ²J_{C-P} = 14 Hz, C^{ipso} Cy), 36.8 (s, CH₂ cod), 35.1 (d, ³J_{C-P} = 3 Hz, C^m Cy), 31.1 (s, CH₂ cod), 28.7 (d, ²J_{C-P} = 10 Hz, C^o Cy), 26.5 (s, C^p Cy). MS (ESI⁺): *m/z* 995.2 (M⁺ + 1H). Anal. Calcd (%) for C₄₀H₆₈Ir₂P₂: C 48.27, H 6.89; found: C 48.13, H 6.57.

[{Ir(μ-PⁱPr₂)(cod)}₂] (7)

A Young NMR tube was charged with 5 (15 mg), dissolved in [D₈]toluene (0.4 mL) and then sealed under argon. On heating the mixture at 40 °C for 12 hours, complete conversion to 7 was achieved. *Td-Pc isomer*: ¹H NMR (300 MHz, C₆D₆): δ 4.03 (m, 4H), 3.80 (m, 4H) (=CH cod), 2.93 (m, 2H), 2.32 (m, 2H) (CHⁱPr), 2.30 (m, 4H), 2.10 (m, 4H), 1.96 (m, 4H), 1.69 (m, 4H), (CH₂ cod), 1.28 (m, 6H), 0.95 (m, 6H) (CH₃ⁱPr). ³¹P{¹H} NMR (121 MHz, C₆D₆): δ 39.0 (s). ¹³C{¹H} RMN (75 MHz, C₆D₆): δ 79.7 (d, ¹J_{C-Rh} = 11 Hz), 59.6 (m) (=CH cod), 39.8 (d, ²J_{C-Rh} = 4 Hz, CH₂), 35.7 (d, ¹J_{C-P} = 8 Hz, CHⁱPr), 35.6 (s, CH₂ cod), 31.9 (d, ¹J_{C-P} = 14 Hz, CHⁱPr), 30.8 (s), 25.7 (s) (CH₃ⁱPr). *Td-Td isomer*: ¹H NMR (300 MHz, C₆D₆): δ 3.50 (m, 8H; =CH cod), 2.93 (m, 4H; CHⁱPr), 2.42 (8H, m), 1.96 (8H, m) (CH₂ cod), 0.95 (m, 12H, CH₃ⁱPr). ³¹P{¹H} NMR (121 MHz, C₆D₆): δ 230.0 (s). ¹³C{¹H} RMN (75 MHz, C₆D₆): δ 59.5 (m, =CH), 39.8 (s, CH₂) (cod), 36.0 (d, ¹J_{C-P} = 8 Hz, CH), 25.7 (s, CH₃) (ⁱPr). MS (ESI⁺): 837.1 (M⁺ + 1H). Anal. Calcd (%) for C₂₈H₅₂Ir₂P₂: C 40.27, H 6.28; found: C 40.19, H 6.12.

Computational details

The geometry of all structures has been optimized with the G09 program package²⁹ at the DFT level using the B3LYP approximation³⁰ in combination with the 6-31G(d) basis set for H, C, N, and P atoms³¹ and the SDD pseudo-potential³² for Ir. The nature of the stationary points has been confirmed by frequency analysis and intrinsic reaction paths have been traced connecting the transition structures with the respective minima.

Crystal structure determination for complexes 2, 3 and 7. Single crystals of suitable size of 2, 3 and 7 were selected and mounted onto the end of a thin glass fibre using Fomblin perfluoropolyether oil. Manipulation of sample 2 required special care, as it is extremely temperature-sensitive (see below). X-ray diffraction data were collected at 100(2) K on a Bruker APEX II (complexes 2 and 7) and on a Bruker SMART APEX (compound 3) area detector diffractometers with graphite-monochromated MoK α radiation ($\lambda = 0.71073$ Å) by using narrow ω rotations (0.3°). Intensities were integrated and corrected for absorption effect with SAINT³³ and SADABS³⁴ programs, included in the APEX2 package. The structures were solved by direct methods with SHELXS-97.³⁵ Refinement, by full-matrix least squares on F^2 , was performed with SHELXL-97.³⁶ Hydrogen atoms bound to olefinic carbon atoms of the cod fragment in 2 and 3 were included in the model in observed positions, and their isotropic thermal parameters were fixed to 1.2 times the U value of the carbon atoms they are linked to. Particular details of the presence of a solvent and specific refinement details are listed below.

Crystal handling of compound 2. Due to the sensitivity of 2, the sample in its mother liquor was stored in an ordinary Schlenk flask whose crystallization temperature was maintained using a cooling bath. Single crystals were picked out from the mother solution in a small spoon with Fomblin oil. They were quickly immersed in inert oil on a microscope slide with a cavity surrounded by dry-ice blocks. The generated cool inert gas atmosphere maintained the crystal quality.

Crystal data for complex 2. C₄₀H₄₇Ir₂NP₂; $M = 988.21$; orange prism; $0.148 \times 0.141 \times 0.134$ mm³; monoclinic; $P2_1/n$; $a = 10.8643(12)$, $b = 29.946(3)$, $c = 11.1359(13)$ Å; $\beta = 107.334(2)^\circ$; $Z = 4$; $V = 3458.5(7)$ Å³; $\rho_{\text{calc}} = 1.898$ g cm⁻³; $\mu = 7.810$ mm⁻¹; min. and max. transmission factors: 0.317 and 0.461; $2\theta_{\text{max}} = 59^\circ$; 44 776 reflections collected, 9093 unique [$R_{\text{int}} = 0.0450$]; the number of data/restraints/parameters: 9093/2/442; final GoF : 1.035, $R_1 = 0.0282$ [7517 reflections, $I > 2\sigma(I)$], $wR_2 = 0.0606$ for all data; the largest difference peak: 1.838 e Å⁻³. A hydride atom has been observed in the Fourier difference map. It has been included in the model at this observed position and refined with a restraint on the Ir-H distance. At the end of the refinement, nine residual density peaks higher than 1 e Å⁻³ were found. All of them are close to the metal atoms. They have no chemical sense.

Crystal data for complex 3. C₄₀H₄₇Ir₂NP₂·C₆D₆; $M = 1072.35$; red prism; $0.258 \times 0.111 \times 0.110$ mm³; orthorhombic; $Pbca$; $a = 21.7209(10)$, $b = 10.3274(5)$, $c = 33.4874(16)$ Å; $Z = 8$; $V = 7511.9(6)$ Å³; $\rho_{\text{calc}} = 1.896$ g cm⁻³; $\mu = 7.199$ mm⁻¹; min. and max. transmission factors: 0.242 and 0.446; $2\theta_{\text{max}} = 57.08^\circ$; 85 822 reflections collected, 9153 unique [$R_{\text{int}} = 0.0456$]; the number of data/restraints/parameters: 9153/19/431; final GoF : 1.214, $R_1 = 0.0419$ [8274 reflections, $I > 2\sigma(I)$], $wR_2 = 0.0871$ for all data; the largest difference peak: 1.674 e Å⁻³. A disorder has been observed in four carbon atoms of both cod-based ligands (C₈H₁₂ and C₈H₁₃ fragments). They have been included in the model in two sets of positions with complementary occupancy factors (0.7/0.3). They have been refined with geometrical

restraints. Hydrogen atoms of the NH₂ bridging group have been included in the model in observed positions and refined with a restraint on N–H distances. They are very large solvent accessible voids in the structure and a zone where residual density peaks are observed. The solvent is highly disordered and could not be properly modelled. Therefore, SQUEEZE³⁷ corrections have been applied. The total potential solvent accessible void volume and the electron count may agree with the presence of eight C₆D₆ molecules.

Crystal data for complex 7. C₂₈H₅₂Ir₂P₂; *M* = 835.11; red prism; 0.281 × 0.114 × 0.111 mm³; monoclinic; *P*₂/c; *a* = 12.0438(6), *b* = 13.3654 (6), *c* = 17.5773(8) Å; β = 95.2757(6)°; *Z* = 4; *V* = 2817.4(2) Å³; ρ_{calc} = 1.968 g cm⁻³; μ = 9.559 mm⁻¹; min. and max. transmission factors: 0.185 and 0.331; 2θ_{max} = 54.96°; 27 939 reflections collected, 6455 unique [*R*_{int} = 0.0277]; the number of data/restraints/parameters: 6455/1/409; final *GoF*: 1.032, *R*₁ = 0.0173 [5340 reflections, *I* > 2σ(*I*)], w*R*₂ = 0.0400 for all data; the largest difference peak: 0.974 e Å⁻³. Hydrogen atoms of methyl groups have been included in the model at calculated positions and refined with a riding model. The rest of the hydrogen atoms have been included in the model at observed positions and freely refined. Only one restraint on a C–H distance has been included in the refinement.

Acknowledgements

Financial support from the project CTQ2012-35665 and the CONSOLIDER INGENIO-2010 program under the projects MULTICAT (CSD2009-00050) and Factoría de Cristalización (CSD2006-0015), and DGA/FSE 07, is acknowledged. P.G.O. acknowledges the CSIC “JAE-Doc” program, cofunded by the ESF and Factoría de Cristalización projects, for financial support. The author V.P. thankfully acknowledges the resources from the supercomputer “Terminus”, and the technical expertise and assistance provided by the Institute for Biocomputation and Physics of Complex Systems (BIFI) – Universidad de Zaragoza.

Notes and references

- (a) A. L. Gavrilovaa and B. Bosnich, *Chem. Rev.*, 2004, **104**, 349; (b) L. A. Oro, M. A. Ciriano and C. Tejel, *Pure Appl. Chem.*, 1998, **70**, 779.
- For selected examples on dinuclear cooperative activation, see: (a) T. S. Teets, T. R. Cook, B. D. McCarthy and D. G. Nocera, *Inorg. Chem.*, 2011, **50**, 5223; (b) Y. Takahashi, M. Nonogawa, K. Fujita and R. Yamaguchi, *Dalton Trans.*, 2008, 3546; (c) T. Shima and H. Suzuki, *Organometallics*, 2005, **24**, 3939; (d) K. Fujita, H. Nakaguma, T. Hamada and R. Yamaguchi, *J. Am. Chem. Soc.*, 2003, **125**, 12368; (e) Y. Yuan, M. V. Jiménez, E. Sola, F. J. Lahoz and L. A. Oro, *J. Am. Chem. Soc.*, 2002, **124**, 752; (f) M. V. Jiménez, E. Sola, J. Caballero, F. J. Lahoz and L. A. Oro, *Angew. Chem., Int. Ed.*, 2002, **41**, 1208; (g) T. Shima and H. Suzuki, *Organometallics*, 2000, **19**, 2420; (h) D. Ristic-Petrovic, J. R. Torkelson, R. W. Hilt, R. McDonald and M. Cowie, *Organometallics*, 2000, **19**, 4432; (i) D. A. Vicić and W. D. Jones, *Organometallics*, 1999, **18**, 134; (j) J. R. Torkelson, F. H. Antwi-Nsiah, R. McDonald, M. Cowie, J. G. Pruis, K. J. Jalkanen and R. L. DeKock, *J. Am. Chem. Soc.*, 1999, **121**, 3666; (k) H. Suzuki, H. Omori, D. H. Lee, Y. Yoshida, M. Fukushima, M. Tanaka and Y. Moro-oka, *Organometallics*, 1994, **13**, 1129; (l) D. A. Vicić and W. D. Jones, *Organometallics*, 1997, **16**, 1912; (m) W. D. McGhee, F. J. Hollander and R. G. Bergman, *J. Am. Chem. Soc.*, 1988, **110**, 8428.
- See for example: (a) V. Miranda-Soto, J. J. Pérez-Torrente, L. A. Oro, F. J. Lahoz, M. L. Martín, M. Parra-Hake and D. B. Grotjahn, *Organometallics*, 2006, **25**, 4374; (b) S. Matsukawa, S. Kuwata and M. Hidai, *Inorg. Chem.*, 2000, **39**, 791; (c) M. Nishio, H. Matsuzaka, Y. Mizobe and M. Hidai, *Inorg. Chim. Acta*, 1997, **263**, 119; (d) F. A. Cotton, P. Lahuerta, J. Latorre, M. Sanati, I. Solaria and W. Schwotze, *Inorg. Chem.*, 1988, **27**, 2131; (e) C. Claver, J. Fis, P. Kalck and J. Jaud, *Inorg. Chem.*, 1987, **26**, 3479; (f) P. Kalck and J. J. Bonnet, *Organometallics*, 1982, **1**, 1211.
- (a) P. García-Orduña, M. A. Casado, I. Mena and F. J. Lahoz, *Acta Crystallogr., Sect. C: Cryst. Struct. Commun.*, 2012, **68**, m113; (b) S. Takemoto, T. Honma and H. Matsuzaka, *Organometallics*, 2011, **30**, 1013; (c) C. Tejel, M. A. Ciriano, M. Bordonaba, J. A. López, F. J. Lahoz and L. A. Oro, *Inorg. Chem.*, 2002, **41**, 2348; (d) L. A. Oro, D. Carmona, M. P. Lamata, M. C. Apreada, C. Foces-Foces, F. H. Cano and P. M. Maitlis, *J. Chem. Soc., Dalton Trans.*, 1984, 1823; (e) M. P. García, M. V. Jiménez, T. Luengo and L. A. Oro, *J. Organomet. Chem.*, 1996, **510**, 189.
- (a) C. Tejel, M. A. Ciriano, J. A. López, S. Jiménez, M. Bordonaba and L. A. Oro, *Chem.–Eur. J.*, 2007, **13**, 2044; (b) C. Tejel, M. A. Ciriano, M. Bordonaba, J. A. López, F. J. Lahoz and L. A. Oro, *Chem.–Eur. J.*, 2002, **8**, 3128; (c) S. Kannan, A. J. James and P. R. Sharp, *Inorg. Chim. Acta*, 2000, **19**, 155; (d) J. Brunet, J.-C. Daran, D. Neibecker and L. Rosenberg, *J. Organomet. Chem.*, 1997, **538**, 251; (e) M. K. Kolel-Veetil, A. L. Rheingold and K. J. Ahmed, *Organometallics*, 1993, **12**, 3439; (f) M. K. Kolel-Veetil, M. Rahim, A. J. Edwards, A. L. Rheingold and K. J. Ahmed, *Inorg. Chem.*, 1992, **31**, 3877.
- (a) I. Mena, E. A. Jaseer, M. A. Casado, P. García-Orduña, F. J. Lahoz and L. A. Oro, *Chem.–Eur. J.*, 2013, **19**, 5665; (b) P. Kläring, S. Pahl, T. Braun and A. Penner, *Dalton Trans.*, 2011, **40**, 6785; (c) M. A. Salomon, A.-K. Jungton and T. Braun, *Dalton Trans.*, 2009, 7669; (d) T. Kimura, H. Arita, K. Ishiwata, S. Kuwata and T. Ikariya, *Dalton Trans.*, 2009, 2912; (e) R. Koelliker and D. Milstein, *Angew. Chem., Int. Ed.*, 1991, **30**, 907; (f) A. L. Casalnuovo, J. C. Calabrese and D. Milstein, *Inorg. Chem.*, 1987, **26**, 971.
- For homolytic splitting of ammonia leading to parent amido complexes, see: (a) E. Morgan, D. F. MacLean, R. McDonald and L. Turculet, *J. Am. Chem. Soc.*, 2009, **131**,

- 14234; (b) C. M. Fafard, D. Adhikari, B. M. Foxman, D. J. Mindiola and O. V. Ozerov, *J. Am. Chem. Soc.*, 2007, **129**, 10318; (c) J. Zhao, A. S. Goldman and J. F. Hartwig, *Science*, 2005, **307**, 1080.
- 8 For heterolytic splitting of ammonia leading to parent amido complexes, see: (a) I. Mena, M. A. Casado, P. García-Orduña, V. Polo, F. J. Lahoz, A. Fazal and L. A. Oro, *Angew. Chem., Int. Ed.*, 2011, **50**, 11735; (b) T. Kimura, N. Koiso, K. Ishiwata, S. Kuwata and T. Ikariya, *J. Am. Chem. Soc.*, 2011, **133**, 8880; (c) T. Khaskin, M. A. Iron, L. J. W. Shimon, J. Zhang and D. Milstein, *J. Am. Chem. Soc.*, 2010, **132**, 8542; (d) C. Ni, H. Lei and P. P. Power, *Organometallics*, 2010, **29**, 1988; (e) J. J. Li, W. Li, A. J. James, T. Holbert, T. P. Sharp and P. R. Sharp, *Inorg. Chem.*, 1999, **38**, 1563.
- 9 (a) J. L. Klinkenberg and J. F. Hartwig, *Angew. Chem., Int. Ed.*, 2011, **50**, 86; (b) T. Braun, *Angew. Chem., Int. Ed.*, 2005, **44**, 5012; (c) J. I. van der Vlugt, *Chem. Soc. Rev.*, 2010, **39**, 2302; (d) Y. Aubin, C. Fischmeister, C. M. Thomas and J. L. Renaud, *Chem. Soc. Rev.*, 2010, **39**, 4130.
- 10 (a) J. Zhou and J. F. Hartwig, *Angew. Chem., Int. Ed.*, 2008, **47**, 5783; (b) D. Conner, K. N. Jayaprakash, T. R. Cundari and T. B. Gunnoe, *Organometallics*, 2004, **23**, 2724; (c) D. J. Fox and R. G. Bergman, *J. Am. Chem. Soc.*, 2003, **125**, 8984; (d) K. N. Jayaprakash, D. Conner and T. B. Gunnoe, *Organometallics*, 2001, **20**, 5254.
- 11 I. Mena, M. A. Casado, V. Polo, P. García-Orduña, F. J. Lahoz and L. A. Oro, *Angew. Chem., Int. Ed.*, 2012, **51**, 8259.
- 12 G. W. Bushnell, M. A. Casado and S. R. Stobart, *Organometallics*, 2001, **20**, 601.
- 13 O. Kühn, *Phosphorus-31 NMR Spectroscopy: A Concise Introduction for the Synthetic Organic and Organometallic Chemist*, Springer, Germany, 2008.
- 14 L. A. Oro, E. Sola, J. A. López, F. Torres, A. Elduque and F. J. Lahoz, *Inorg. Chem. Commun.*, 1998, **1**, 64.
- 15 (a) T. Shima, Y. Sugimura and H. Suzuki, *Organometallics*, 2009, **28**, 871; (b) G. W. Bushnell, S. R. Stobart, R. Vefghi and M. J. Zaworoto, *J. Chem. Soc., Chem. Commun.*, 1984, 282.
- 16 P. E. Kreter and D. W. Meek, *Inorg. Chem.*, 1983, **22**, 319.
- 17 M. Martín, E. Sola, O. Torres, P. Plou and L. A. Oro, *Organometallics*, 2003, **22**, 5406.
- 18 The complex $[\text{Co}(\eta^4\text{-cod})_2(\text{H})]$ has been found to be in labile equilibrium with the product resulting from a hydrido migratory insertion $[\text{Co}(\eta^4\text{-cod})(1-\kappa\text{-}4,5\text{-}\eta^2\text{-C}_8\text{H}_{13})]$, see: S. Otsuka and M. Rossi, *J. Chem. Soc. A*, 1968, 2530.
- 19 (a) G. A. Silantyev, O. A. Filippov, P. M. Tolstoy, N. V. Belkova, L. M. Epstein, K. Weisz and E. S. Shubina, *Inorg. Chem.*, 2013, **52**, 1787; (b) O. A. Filippov, N. V. Belkova, L. M. Epstein, A. Lledós and E. S. Shubina, *Comput. Theor. Chem.*, 2012, **998**, 129; (c) M. Baya, O. Maresca, R. Poli, Y. Coppel, F. Maseras, A. Lledós, N. V. Belkova, P. A. Dub, L. M. Epstein and E. S. Shubina, *Inorg. Chem.*, 2006, **45**, 10248; (d) N. V. Belkova, P. O. Revin, L. M. Epstein, E. V. Vorontsov, V. I. Bakhmutov, E. S. Shubina, E. Collange and R. Poli, *J. Am. Chem. Soc.*, 2003, **125**, 11106.
- 20 For catalytic isomerizations promoted by hydrido late metal complexes, see for example: (a) S. Biswas, Z. Huang, Y. Choliy, D. Y. Wang, M. Brookhart, K. Krogh-Jespersen and A. S. Goldman, *J. Am. Chem. Soc.*, 2012, **134**, 13276; (b) A. Scarso, M. Colladon, P. Sgarbossa, C. Santo, R. A. Michelin and G. Strukul, *Organometallics*, 2010, **29**, 1847; (c) R. H. Crabtree, in *The Organometallic Chemistry of the Transition Metals*, John Wiley & Sons, Hoboken, NJ, 5th edn, 2009, pp. 229–231; (d) P. W. N. M. van Leeuwen, in *Homogeneous Catalysis*, Kluwer Academic Publishers, Dordrecht, 2004, pp. 101–105.
- 21 (a) T. S. Targos, G. L. Geoffroy and A. L. Rheingold, *Organometallics*, 1986, **5**, 12; (b) E. W. Burkhardt, W. C. Mercer and G. L. Geoffroy, *Inorg. Chem.*, 1984, **23**, 1779; (c) R. A. Jones, N. C. Norman, M. H. Seeberger, J. L. Atwood and W. E. Hunter, *Organometallics*, 1983, **2**, 1629; (d) R. A. Jones, T. C. Wright, J. L. Atwood and W. E. Hunter, *Organometallics*, 1983, **2**, 470; (e) D. W. Meek, P. E. Kreter and G. G. Christoph, *J. Organomet. Chem.*, 1982, **231**, C53; (f) R. A. Jones and T. C. Wright, *Organometallics*, 1983, **2**, 1842.
- 22 H. A. Jenkins, S. J. Loeb and N. T. McManus, *Inorg. Chim. Acta*, 1989, **159**, 83–86.
- 23 (a) P. L. Bellon, C. Benedicenti, G. Caglio and M. Manassero, *J. Chem. Soc., Chem. Commun.*, 1973, 946; (b) R. Mason, I. Sotofte, S. D. Robinson and M. F. Uttley, *J. Organomet. Chem.*, 1972, **46**, C61.
- 24 A. M. Arif, D. E. Heaton, R. A. Jones, K. B. Kidd, T. C. Wright, B. R. Whittlesey, J. L. Atwood, W. E. Hunter and H. Zhang, *Inorg. Chem.*, 1987, **26**, 4065.
- 25 (a) J. B. Bleeker, A. M. Rohde and K. D. Robinson, *Organometallics*, 1995, **14**, 1674; (b) J. B. Bleeker, A. M. Rohde and K. D. Robinson, *Organometallics*, 1994, **13**, 401.
- 26 S.-K. Kang, T. A. Albright, T. C. Wright and R. A. Jones, *Organometallics*, 1985, **4**, 666.
- 27 Reported examples of reductive elimination of ammonia on late metal complexes: (a) M. Morgan, D. F. MacLean, R. McDonald and L. Turculett, *J. Am. Chem. Soc.*, 2009, **131**, 14234; (b) J. Zhao, A. S. Goldman and J. F. Hartwig, *Science*, 2005, **307**, 1080; (c) D. Conner, K. N. Jayaprakash, T. R. Cundari and T. B. Gunnoe, *Organometallics*, 2004, **23**, 2724; (d) M. Kanzelberger, X. Zhang, T. J. Emge, A. S. Goldman, J. Zhao, C. Incarvito and J. F. Hartwig, *J. Am. Chem. Soc.*, 2003, **125**, 13644; (e) S. Park, D. M. Roundhill and A. L. Rheingold, *Inorg. Chem.*, 1987, **26**, 3972; only one example of reductive elimination of primary arylamines from palladium parent amido complexes has been reported, see: J. L. Klinkenberg and J. F. Hartwig, *J. Am. Chem. Soc.*, 2010, **132**, 11830.
- 28 A. Wawer and I. Wawer, *J. Chem. Soc., Perkin Trans. 2*, 1990, 2045.
- 29 M. J. Frisch, *et al.*, *Gaussian 09, revision A.1*, Gaussian, Inc., Wallingford, CT, 2004. The full reference is given in the ESI.†

- 30 (a) A. D. Becke, *J. Chem. Phys.*, 1993, **98**, 1372; (b) C. Lee, W. Yang and R. G. Parr, *Phys. Rev. B: Condens. Matter*, 1988, **37**, 785; (c) A. D. Becke, *J. Chem. Phys.*, 1993, **98**, 5648.
- 31 (a) W. J. Hehre, R. Ditchfield and J. A. Pople, *J. Chem. Phys.*, 1972, **56**, 2257; (b) P. C. Hariharan and J. A. Pople, *Theor. Chim. Acta*, 1973, **28**, 213.
- 32 (a) D. Andrae, U. Haussermann, M. Dolg, H. Stoll and H. Preuss, *Theor. Chim. Acta*, 1990, **77**, 123; (b) M. Dolg, H. Stoll, H. Preuss and R. M. Pitzer, *J. Phys. Chem.*, 1993, **97**, 5852.
- 33 *SAINT+*, 6.01, Bruker AXS, Inc., Madison, USA, 2000.
- 34 G. M. Sheldrick, *SADABS program*, University of Göttingen, Göttingen, Germany, 1999.
- 35 (a) G. M. Sheldrick, *Acta Crystallogr., Sect. A: Fundam. Crystallogr.*, 1990, **46**, 467; (b) G. M. Sheldrick, *Methods Enzymol.*, 1997, **276**, 628.
- 36 G. M. Sheldrick, *Acta Crystallogr., Sect. A: Fundam. Crystallogr.*, 2008, **64**, 112.
- 37 P. V. der Luis and A. L. Spek, *Acta Crystallogr., Sect. A: Fundam. Crystallogr.*, 1990, **46**, 194.